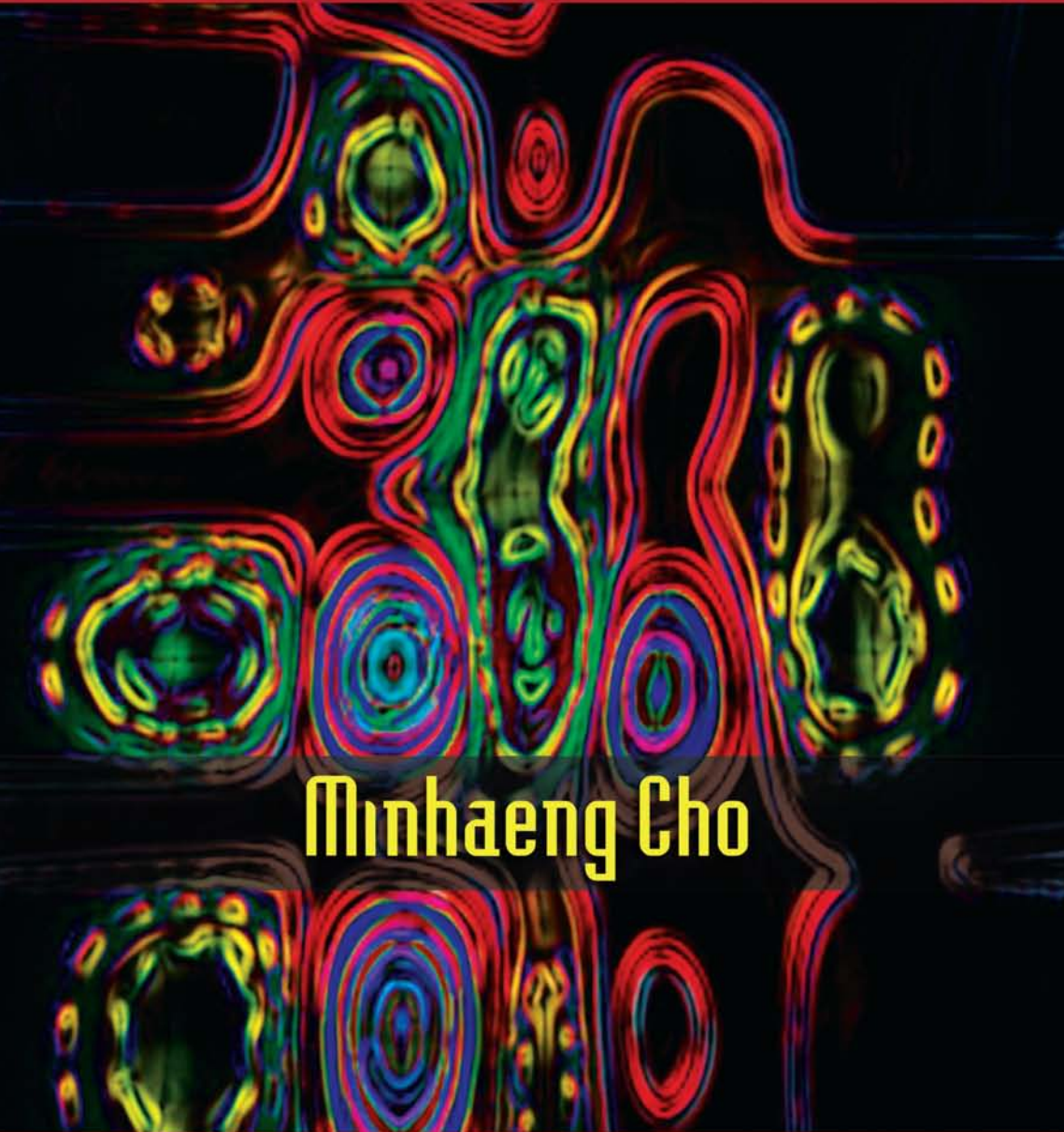


Two-Dimensional Optical Spectroscopy

An abstract, colorful pattern consisting of concentric, wavy lines in shades of red, orange, yellow, green, and blue, set against a dark background. The pattern resembles a complex interference or diffraction pattern, with various shapes and sizes of loops and swirls.

Minhaeng Cho



CRC Press
Taylor & Francis Group

Two-Dimensional Optical Spectroscopy

Two-Dimensional Optical Spectroscopy

Minhaeng Cho



CRC Press

Taylor & Francis Group

Boca Raton London New York

CRC Press is an imprint of the
Taylor & Francis Group, an **informa** business

CRC Press
Taylor & Francis Group
6000 Broken Sound Parkway NW, Suite 300
Boca Raton, FL 33487-2742

© 2009 by Taylor and Francis Group, LLC
CRC Press is an imprint of Taylor & Francis Group, an Informa business

No claim to original U.S. Government works

Printed in the United States of America on acid-free paper
10 9 8 7 6 5 4 3 2 1

International Standard Book Number: 978-1-4200-8429-0 (Hardback)

This book contains information obtained from authentic and highly regarded sources. Reasonable efforts have been made to publish reliable data and information, but the author and publisher cannot assume responsibility for the validity of all materials or the consequences of their use. The authors and publishers have attempted to trace the copyright holders of all material reproduced in this publication and apologize to copyright holders if permission to publish in this form has not been obtained. If any copyright material has not been acknowledged please write and let us know so we may rectify in any future reprint.

Except as permitted under U.S. Copyright Law, no part of this book may be reprinted, reproduced, transmitted, or utilized in any form by any electronic, mechanical, or other means, now known or hereafter invented, including photocopying, microfilming, and recording, or in any information storage or retrieval system, without written permission from the publishers.

For permission to photocopy or use material electronically from this work, please access www.copyright.com (<http://www.copyright.com/>) or contact the Copyright Clearance Center, Inc. (CCC), 222 Rosewood Drive, Danvers, MA 01923, 978-750-8400. CCC is a not-for-profit organization that provides licenses and registration for a variety of users. For organizations that have been granted a photocopy license by the CCC, a separate system of payment has been arranged.

Trademark Notice: Product or corporate names may be trademarks or registered trademarks, and are used only for identification and explanation without intent to infringe.

Library of Congress Cataloging-in-Publication Data

Cho, Minhaeng, 1965-
Two-dimensional optical spectroscopy / Minhaeng Cho.
p. cm.
Includes bibliographical references and index.
ISBN 978-1-4200-8429-0 (hard back : alk. paper)
1. Optical spectroscopy. 2. Quantum optics. I. Title.

QC454.O66C46 2009
535.8'4--dc22

2009015407

Visit the Taylor & Francis Web site at
<http://www.taylorandfrancis.com>

and the CRC Press Web site at
<http://www.crcpress.com>

Table of Contents

Preface.....	ix
About the Author	xi
Acknowledgments.....	xiii
Chapter 1 Introduction	1
References.....	6
Chapter 2 Quantum Dynamics.....	9
2.1 Time Evolution in Hilbert Space	9
2.2 Time-Dependent Perturbation Theory in Hilbert Space	12
2.3 Diagram Representation of the Time-Dependent Perturbation Theory in Hilbert Space	15
2.4 Transition Amplitude and Probability in Hilbert Space	17
2.5 Time Evolution in Liouville Space	20
2.6 Time-Dependent Perturbation Theory in Liouville Space	22
2.7 Transition Probability in Liouville Space and Pathways.....	26
2.7.1 Second-Order Transition between Two Populations	26
2.7.2 Second-Order Transition between Two Coherences	28
2.7.3 First-Order Transition between Population and Coherence	29
References.....	30
Chapter 3 Linear Response Spectroscopy	31
3.1 Linear Response Function	33
3.2 System–Bath Interaction and Line Broadening.....	36
3.3 Rotational Averaging of Tensors.....	45
3.4 Linear Absorption Spectroscopy	47
3.5 Raman Scattering.....	50
3.6 Hyper-Raman Scattering	54
3.7 IR-Raman Surface Vibrational Spectroscopy.....	56
3.8 Raman-IR Surface Vibrational Spectroscopy	59
Appendix: Nonlinear Polarization and Generated Signal Electric Field.....	61
References.....	62

Chapter 4	Second-Order Response Spectroscopy	63
4.1	Second-Order Response Function	64
4.2	Three-Level System and Line-Broadening Function	68
4.3	Sum Frequency Generation.....	75
4.4	Difference Frequency Generation.....	76
4.5	IR–IR-vis Four-Wave Mixing	78
	References.....	80
Chapter 5	Third-Order Response Spectroscopy	83
5.1	Third-Order Response Function	83
5.2	Four-Level System and Line-Broadening Function.....	87
5.3	Short-Time Approximation to the Third-Order Response Function	93
5.4	Third-Order Response Function of a Two-Level System.....	96
5.5	Pump–Probe Spectroscopy of a Two-Level System.....	100
5.6	Rephasing Photon Echo Spectroscopy of a Two-Level System.....	103
5.7	Nonrephasing Photon Echo Spectroscopy of a Two-Level System.....	107
5.8	Three-Pulse Photon Echo Peak Shift (PEPS).....	108
	References.....	112
Chapter 6	Two-Dimensional Pump–Probe Spectroscopy	115
6.1	Introduction to Two-Dimensional Pump–Probe Spectroscopy.....	115
6.2	Two-Dimensional Pump–Probe Spectrum of Two-Level System.....	117
6.3	Two-Dimensional Pump–Probe Spectrum of an Anharmonic Oscillator	123
	References.....	129
Chapter 7	Two-Dimensional Photon Echo Spectroscopy	131
7.1	Phase and Amplitude Detection of the Two- Dimensional Photon Echo Signal Field	132
7.2	Two-Dimensional Photon Echo Spectrum of a Two-Level System.....	135
7.3	Two-Dimensional Nonrephasing Photon Echo Spectrum of a Two-Level System	139
7.4	Two-Dimensional Photon Echo Spectrum of an Anharmonic Oscillator	142

7.5	Simple Two-Dimensional Lorentzian Peak Shape	144
7.6	Simple Two-Dimensional Gaussian Peak Shape	146
	References.....	148
Chapter 8	Coupled Multi-Chromophore System.....	151
8.1	Frenkel Hamiltonian in Site Representation.....	152
8.2	Delocalized Exciton Representation	154
8.3	Delocalized State Energy and Transition Dipole Matrix Element	155
8.4	Transition Frequency–Frequency Correlation Functions.....	157
8.5	Exchange-Narrowing Effect on Absorption Spectrum.....	158
8.6	Measurements of Auto- and Cross-Frequency–Frequency Correlation Functions	160
8.7	Exciton Population Transfer.....	163
	References.....	166
Chapter 9	Two-Dimensional Spectroscopy of Coupled Dimers	169
9.1	Model Hamiltonian of a Coupled Two-Level System Dimer	169
9.2	Delocalized Excited-State Energy Fluctuations and Time Correlation Functions	172
9.3	Coupled Two-Level System Dimer: Quantum Beats at Short Time	174
9.4	Coupled Two-Level System Dimer: Intermediate Time Region.....	179
9.5	Coupled Two-Level System Dimer: Population Transfer Effects.....	181
9.6	Coupled Anharmonic Oscillators: Model Hamiltonian	188
9.7	Coupled Anharmonic Oscillators: Two-Dimensional Photon Echo Spectrum at Short Time	191
9.8	Coupled Anharmonic Oscillators: Degenerate Case	195
9.9	Coupled Anharmonic Oscillators: Population Transfer Effects.....	204
	References.....	207
Chapter 10	Chemical Exchange and Two-Dimensional Spectroscopy	209
10.1	Model System.....	210
10.2	Chemical Exchange Diagrams: Two-Level System.....	212
10.3	Chemical Exchange Diagrams: Anharmonic Oscillator.....	216
	References.....	221

Chapter 11	Polarization-Controlled Two-Dimensional Spectroscopy	223
11.1	Parallel Polarization ZZZZ-Echo: Two-Level System	223
11.2	Perpendicular Polarization ZYYZ-Echo: Two-Level System	228
11.3	Difference Two-Dimensional Photon Echo Spectrum: Coupled Two-Level System Dimer	230
11.4	Parallel Polarization ZZZZ-Echo: Anharmonic Oscillators	231
11.5	Perpendicular Polarization ZYYZ-Echo: Anharmonic Oscillators	233
11.6	Difference Two-Dimensional Echo Spectrum: Coupled Anharmonic Oscillators	235
11.7	Generalized Polarization-Controlled Two-Dimensional Spectroscopy	237
11.8	Determination of the Angle between Any Two Transition Dipole Vectors	240
	References	243
Chapter 12	Applications of Two-Dimensional Vibrational Spectroscopy	245
12.1	Single Anharmonic Oscillator Systems	246
12.2	Coupled Two-Oscillator Systems	253
12.3	Polypeptide Secondary Structures	258
12.4	Globular Proteins and Membrane-Bound Proteins	265
12.5	Nucleic Acids	266
12.6	Hydrogen-Bonding Dynamics and Chemical Exchange	267
12.7	Solute–Solvent Complexation and Micro-Solvation	270
12.8	Internal Rotation	272
12.9	Transient Two-Dimensional IR Spectroscopy: Protein Folding and Unfolding	272
	References	274
Chapter 13	Applications of Two-Dimensional Electronic Spectroscopy	283
13.1	Application to Fenna–Matthews–Olson Light-Harvesting Complex	283
13.2	Application to Semiconductors	289
	References	291
Chapter 14	Two-Dimensional Second-Order Response Spectroscopy	293
14.1	Two-Dimensional Sum Frequency Generation	294
14.2	Two-Dimensional Sum Frequency Generation of Solution Sample	296

14.3	Two-Dimensional Sum Frequency Generation of Coupled Two-Level System Dimer.....	298
14.4	Two-Dimensional Sum Frequency Generation of Coupled Anharmonic Oscillators.....	301
14.5	Two-Dimensional Difference Frequency Generation.....	305
14.6	IR–IR-vis Sum Frequency Generation and Difference Frequency Generation.....	306
14.7	Other IR–IR-vis Four-Wave-Mixings.....	313
14.8	Fifth-Order Raman Scattering.....	316
	References.....	320
Chapter 15	Linear Optical Activity Spectroscopy.....	323
15.1	Radiation–Matter Interaction Hamiltonian and Polarization.....	324
15.2	Circular Dichroism and Optical Rotatory Dispersion.....	326
15.3	Raman Optical Activity.....	334
15.4	IR-Raman Optical Activity Spectroscopy.....	341
15.5	Raman-IR Optical Activity Spectroscopy.....	346
	References.....	350
Chapter 16	Nonlinear Optical Activity Spectroscopy.....	351
16.1	Nonlinear Optical Activity Measurement Methods.....	351
16.2	Rotational Averaging of Higher-Rank Tensors.....	353
16.3	Two-Dimensional Optical Activity Pump–Probe: Two-Level System.....	358
16.4	Two-Dimensional Optical Activity Photon Echo: Two-Level System.....	367
16.5	Two-Dimensional Optical Activity Photon Echo of Coupled Two-Level System Dimer.....	369
	References.....	373
Index.....		375

Preface

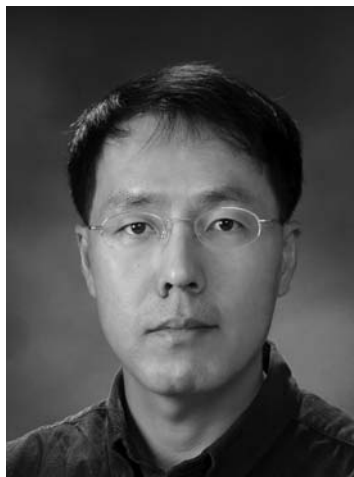
The purpose of this book is twofold: It provides a detailed account of basic theory required for an understanding of the two-dimensional vibrational and electronic spectroscopy, and it also bridges the gap between the formal development of nonlinear optical spectroscopy and the application of the theory to the explanation of experimental results. The main emphasis is on principles rather than on practical aspects, though the reader may find sections where practical applications of the two-dimensional optical spectroscopy to complicated molecular systems, such as proteins and light-harvesting complexes, dominate.

It is assumed that the reader has the usual undergraduate background knowledge of quantum mechanics, electromagnetic theory, spectroscopy, statistical mechanics, and physical chemistry. This book is intended to serve as a monograph for researchers in this particular topic as well as a textbook for advanced graduate students. I hope that it helps to fulfill the needs of time-domain spectroscopists who wish to deepen their understanding of the basic features of nonlinear response function theory and intermolecular interaction-induced phenomena and who intend to apply the recently developed tools of vibrational and electronic spectroscopy in two dimensions.

The scope of the material is restricted in various ways, but most importantly, theoretical descriptions of two-dimensional spectroscopy of coupled two-level systems and anharmonic oscillators are generally valid and can be easily extended to account for the two-dimensional spectroscopy of coupled multi-chromophore systems.

About the Author

Minhaeng Cho was born in Seoul. He received a BS and an MS in chemistry from Seoul National University in 1987 and 1989, and a PhD from the University of Chicago in 1993 under the direction of Graham R. Fleming. After his post-doctoral training at Massachusetts Institute of Technology in Robert J. Silbey's group from 1994 to 1996, he joined the faculty of Korea University and has been there since March of 1996. He is currently director of the Center for Multidimensional Spectroscopy. His areas of research interest are in theoretical and computational chemistry and ultrafast nonlinear optical spectroscopy.



Acknowledgments

I am grateful to many friends, colleagues, collaborators, graduate students, and postdoctoral researchers, past and present. I am in debt to Jeffrey Cina and Jonggu Jeon for their critical readings of the manuscript, which resulted in many changes and corrections. I would like to express my deep gratitude to those who taught me about the fundamental principles of nonlinear optical spectroscopy, guided my interests toward time domain spectroscopy, corrected misconceptions, and carried out fruitful collaborations: Graham R. Fleming, Shaul Mukamel, Richard M. Stratt, Iwao Ohmine, Robert J. Silbey, Shinji Saito, Yoshitaka Tanimura, Mischa Bonn, Andrei Tokmakoff, John C. Wright, Michael D. Fayer, Hogyu Han, and Seung-Joon Jeon. I wish to thank many scientists around the world for stimulating discussions and clarifying concepts. Finally, I owe special thanks to the production editor, Tara Nieuwesteeg, and the CRC Press staff for their help and encouragement.

1 Introduction

Two-dimensional (2D) optical spectroscopy is an optical analog of 2D nuclear magnetic resonance (NMR) and utilizes multiple ultrashort laser pulses in infrared or UV-visible (vis) frequency range. It has been used to study protein structure and dynamics, hydrogen-bonding dynamics in solutions, femtosecond solvation dynamics, solute-solvent complexation, chemical reaction and exchange dynamics, excitation migration process in photosynthetic light-harvesting complexes, exciton dynamics in semiconductors, and coherence transfers in electronically coupled multi-chromophore systems.¹⁻¹⁹ Due to dramatic advancements of ultrafast laser technologies, femtosecond laser systems operating in infrared and visible frequency ranges have been commercially available so that we have seen a wide range of applications utilizing such ultrafast nonlinear optical spectroscopic techniques.

Most of the conventional linear spectroscopic methods, though they have been proven to be extremely useful for studying structural and dynamical properties of complex molecules in condensed phases, provide highly averaged information. Therefore, novel spectroscopic techniques capable of providing much higher information content have been sought and tested incessantly. In the research community of NMR spectroscopy, such efforts led to developing a variety of 2D NMR techniques such as NOESY (nuclear Overhauser enhancement spectroscopy) and COSY (correlation spectroscopy) methods among many others, and they have been extensively used to study structural and dynamical properties of proteins in solutions.^{1, 2}

Although the 2D optical spectroscopy that has been considered to be an optical analog of 2D NMR does not provide atomic resolution structures of complex molecules, optical domain multidimensional spectroscopy has certain advantages because of the dramatic gain in time resolution (~ subpicosecond scale) possible and the ability to directly observe and quantify the couplings between quantum states involved in molecular dynamical processes.¹⁹ An elementary and highly simplified schematic diagram in Figure 1.1 demonstrates that time-resolved 2D vibrational spectroscopic technique can provide detailed information on the 3D structure of a given complex molecule, that is, proteins.²⁰ A pair of vibrational chromophores, for example, amide I local modes in polypeptide backbone, are coupled to each other via hydrogen-bonding interaction, which results in cross-peaks in the 2D amide I infrared (IR) spectrum. As a molecule undergoes a structural transition along a certain reaction (folding or unfolding) coordinate, where hydrogen-bond breaking occurs, the cross-peaks will disappear in time.²¹ Consequently, the transient 2D vibrational spectroscopy will provide information on the local conformational change of the target molecule in this case.

As theoretically and experimentally demonstrated over the last decade, the existence of cross-peaks is direct evidence on the vibrational couplings whose magnitudes depend on relative distances and orientations between vibrational chromophores

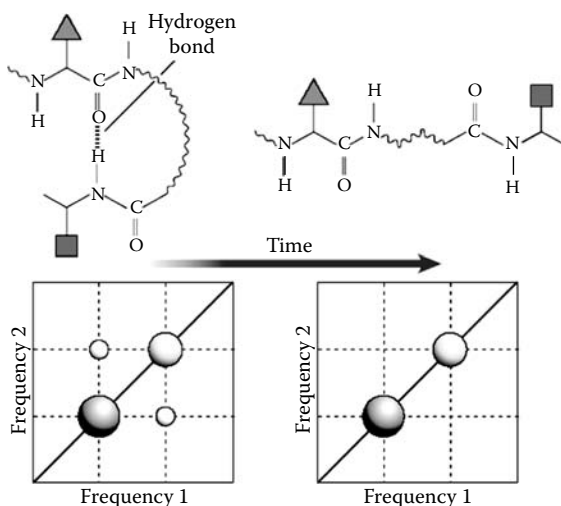


FIGURE 1.1 Two-dimensional spectroscopy of changes in molecular structure. The peaks on the diagonal line of this typical 2D infrared spectrum are associated with vibrations of the chemical groups in red and blue in the structures above (the square and the triangle represent amino acid side groups). The cross-peaks in green are produced by the coupling of these vibrations. As the molecule unfolds, the length of the hydrogen bond increases and the vibrational coupling decreases, so that the cross-peaks become less intense. The cross-peaks disappear when the hydrogen bond is broken. By examining the amplitudes of cross-peaks from a series of time-resolved spectra, the breaking of a hydrogen bond, and so the structural evolution of a small molecule, can be probed in time.

that are comparatively localized anharmonic oscillators.¹⁰ Similarly, if two optical chromophores absorbing UV-vis lights are spatially close to each other, the electronic transition coupling between the two induces an electronic exciton formation and produces cross-peaks in the 2D electronic spectrum.²² Therefore, experimental observation of cross-peaks in a measured 2D electronic spectrum and their transient behaviors in time provides invaluable information about electronic coupling strength between two chromophores and about exciton-exciton coherence and population transfers or even on structural changes.^{9, 22, 23}

Ultrafast nonlinear optical spectroscopy utilizing IR and/or visible field has been a vital and incisive tool with a rich and long history, and an optical analog of NMR phase coherent multiple pulse spectroscopy was alluded before, where the acousto-optic modulation technique was used to generate an optical pulse sequence for a photon echo experiment.³ Particularly, optical photon echo spectroscopy has been extensively used to study solvation dynamics and ultrafast inertial motions of both degrees of freedom coupled to electronic transitions of chromophores in condensed phases.^{24, 25} An IR photon echo experiment utilizing a free electron laser was performed in early 1990s.²⁶ Since the photon echo spectroscopy involves two either vibrational or electronic coherence evolutions during τ and t periods that are separated by another delay time T , the measured echo signal is expressed as $S(t, T, \tau)$.

The 2D spectrum $\tilde{S}(\omega_t, T, \omega_\tau)$ can therefore be obtained by carrying out double Fourier transformations of $S(t, T, \tau)$ with respect to τ and t . T is the so-called waiting time during which the system density matrix element is one of the diagonal elements (populations) or off-diagonal elements (coherences).

A typical 2D spectrum $\tilde{S}(\omega_t, T, \omega_\tau)$ thus obtained exhibits a variety of peaks. There are diagonal and off-diagonal peaks revealing different dynamics of the complex system of interest. For a two-level system, the 2D shape of a diagonal peak provides information on the relative contributions from the inhomogeneous and homogeneous dephasing processes.^{27, 28} The extent of elongation along the diagonal and the slope of the elongation direction are often time-dependent, and their changes were found to be related to the transition frequency–frequency time–correlation function, which is in turn related to the associated solvation dynamics around the chromophore.^{10, 28} For an anharmonic oscillator, which can be successfully modeled as a three-level system, the diagonal peak in the real part of the 2D photon echo spectrum is divided into two parts with positive and negative amplitudes, which reveals overtone anharmonicity. Here, it should be noted that the target oscillators should not be perfectly harmonic to make the associated nonlinear response function nonvanishing. Certain nonlinearities in nuclear and electronic motions are basic requirements. In a given 2D spectrum of anharmonic oscillator, the negative peak corresponds to the excited state absorption contribution to the signal and the positive peak to the sum of ground state bleaching and stimulated emission contributions. The cross-peaks can also be either antidiagonally or diagonally elongated, which corresponds to the cases when the two different transition frequencies are negatively or positively correlated in time. For a coupled homo- or hetero-dimer system, a negative correlation can be induced by modulation of the coupling constant, and a positive correlation results from modulation of the transition frequencies of the two monomers. The intensities of the cross-peaks can change in time, and their time-dependencies originate from various processes such as excitation transfers between two different excitonic or monomeric states, coherence transfers, chemical exchanges and reactions, population-dependent dephasing processes, conformation and chemical structural transitions, and so forth.¹⁰ Thus, any 2D optical spectrum has undoubtedly high information content and uniquely provides underlying dynamics and mechanisms of chemical or physical processes considered.

By using femtosecond IR pulses and dispersive pump–probe spectroscopic technique, 2D IR spectroscopic measurements of proteins in solution were performed in 1998.⁴ Also, interesting combinations of IR and visible beams together to carry out IR-vis four-wave-mixing experiments were theoretically suggested in the late 1990s and shown to be useful in studying electric and mechanical anharmonicity-induced couplings between two different vibrational modes in 1999 experimentally.^{6, 8, 11, 29, 30} This is analogous to the heteronuclear NMR spectroscopy, since both vibrational (bosonic) and electronic (fermionic) degrees of freedom and their couplings were under investigation. Also, electronic photon echo signals from a dye molecule or a photosynthetic light-harvesting protein complex were experimentally measured by using a Fourier transform (FT) spectral interferometry employing the Mach–Zehnder interferometer.^{7, 9} In the latter case, it was found that ultrafast excitation relaxations within the manifold of one-exciton states and coherence evolution in

electronically coupled multi-chromophore systems could be studied by examining the time-dependent changes of the 2D photon echo spectrum and by measuring the cross-peak amplitude changes in time T .²² A conditional probability of finding the system on a specific quantum state ψ_k at a later time when it was initially on a different state ψ_j was found to be the key factor determining the time-dependency of the associated cross-peak amplitude at $(\omega_i = \omega_k, \omega_\tau = \omega_j)$.¹⁹ In addition, we have seen 2D IR spectroscopic studies of chemical exchange dynamics and hydrogen-bond network in water.^{31–37} These works clearly demonstrated how such novel spectroscopic methods can be of use in studying fundamental solute-solvent interaction dynamics in real time with an unprecedented time resolution that cannot be reached by any other spectroscopic means. Technically, a femtosecond collinear phase-coherent 2D spectroscopy and a single-shot 2D pump-probe spectroscopy were experimentally demonstrated, which will speed up data collection times and extend applications of the technique to a wide variety of problems.^{38–40} In parallel with these experimental efforts, numerous theoretical and computational methods combining molecular dynamics (MD) simulation, quantum chemistry calculation, quantum mechanical/molecular mechanical (QM/MM) simulation, and hybrid QM/MD simulation have been developed to accurately simulate the 2D vibrational and electronic spectra of complicated molecular systems such as proteins, nucleic acids, and light-harvesting complexes over the last decade.¹⁰

Before we close this chapter, it would be interesting to provide a viewpoint on how and why the 2D optical spectroscopy is a better tool for studying molecular structure and dynamics, in comparison with the other linear or quasi-linear spectroscopy. Note that the time-resolved spectroscopy capable of recording 1D spectra with respect to time is considered to be quasi-linear spectroscopy because quantitative information on couplings still cannot be directly provided. The discussion on this begins with comparing the hierarchy of protein structures with that of spectroscopic properties. Linear spectroscopy such as IR absorption and Raman scattering can provide critical information on the distribution of vibrational modes in a given polyatomic molecule. There are a variety of marker bands in an IR absorption spectrum of polyatomic molecule. Analysis of IR absorption spectrum of an unknown molecule can thus provide information on the constituent chemical groups and bonds included in the molecule. However, if these vibrational chromophores interact or couple to produce delocalized vibrational states, the linear absorption spectrum provides limited information on such coupling strengths that are however keenly dependent on the 3D structure such as inter-chromophore distances and orientations. Thus, the 2D vibrational spectroscopy capable of measuring such small quantities can be an incisive tool to shed light on the detailed structure and its structural change in time.

In Figure 1.2, there is an interesting analogy between various levels of spectroscopic properties and hierarchical protein structures.^{10, 18, 20} The primary structure of protein is nothing but a sequence of amino acids encoded in the corresponding gene. The relevant energy associated with the primary protein structure formation is the covalent bond energy, that is, peptide bond, of which magnitude is about 100 kJ/mol. The secondary protein structures such as α -helix, β -sheet, β -hairpin, and so forth are mainly determined by the relatively weak hydrogen bonds with energy of about 10 kJ/mol. The protein tertiary (domain) structure formation involves a

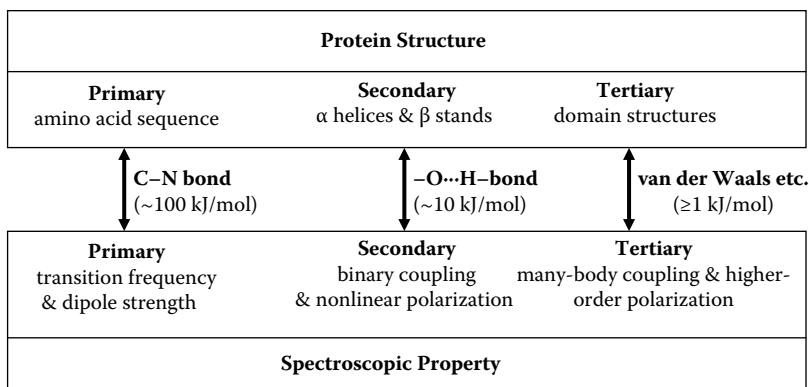


FIGURE 1.2 Analogy between hierarchies of spectroscopic properties and protein structures.

variety of interactions such as electrostatic, hydrophobic, van der Waals, disulfide bond interactions and the like. Thus, the protein structure hierarchy can be viewed as a descending order of interaction energy. Similarly, one can develop the same hierarchical concept for spectroscopically measurable properties. The primary spectroscopic properties are fundamental transition frequencies and transition dipole strengths that are principal quantities extracted from an analysis of 1D spectrum, and such primary spectroscopic properties are largely determined by the nature of covalent bonds involved in a given vibrational (or electronic) chromophore, (e.g., C=O stretch, C-H stretch and bend). Most of the 1D spectroscopic means are consequently very useful in delineating the distribution of individual chromophore in the target molecule, and thus they can be considered to be a *one-body* spectroscopy identifying each single chromophore. On the other hand, the coupling between two different chromophores (electronic or vibrational oscillators) within a molecule is associated with comparatively weak inter-chromophore interactions such as hydrogen bond. Consequently, the secondary spectroscopic properties (e.g., vibrational or electronic couplings, nonlinear optical strengths, anharmonic couplings) require nonzero two-body interactions between different chromophores and thus are very sensitive to the detailed configuration, that is, 3D structure, of the constituent chromophores in the molecule. As has been shown over the last decade, the coherent 2D optical spectroscopy based on a variety of nonlinear optical spectroscopic techniques is superior to the 1D method in extracting such quantitatively small secondary spectroscopic properties of complicated molecules like proteins and molecular aggregates via measuring the two-body interaction terms. Thus, the 2D spectroscopy can be considered as *two-body* spectroscopy. Extending this analogy further, one can envisage the 3D (*three-body*) spectroscopy, which is likely to be of use in measuring the tertiary spectroscopic properties such as three-body (three-chromophore) couplings and higher-order nonlinear optical strengths, as a technique that enables determination of higher-order hierarchical molecular structure.

In this book, we will provide detailed discussions on the underlying physics and interpretation methods of a variety of 2D optical spectroscopic methods. Novel

diagrammatic techniques will be presented and shown to be useful in graphically describing the associated nonlinear optical transition pathways and involved population (diagonal density matrix elements) or coherence (off-diagonal density matrix elements) evolutions. The basics of quantum dynamics are explained first, and time-dependent perturbation theories that are required in describing nonlinear optical processes. Although a number of nonlinear spectroscopic investigations have been performed in frequency domain, we will focus on time-domain spectroscopy only because it is far more suitable for describing ultrafast coherent 2D optical measurements as well as directly analogous to the 2D NMR spectroscopy in many ways.

REFERENCES

1. Ernst, R. R.; Bodenhausen, G.; Wokaun, A., *Nuclear magnetic resonance in one and two dimensions*. Oxford University Press: Oxford, 1987.
2. Wüthrich, K., *NMR of proteins and nucleic acids*. John Wiley & Sons: New York, 1986.
3. Warren, W. S.; Zewail, A. H., Optical analogs of NMR phase coherent multiple pulse spectroscopy. *Journal of Chemical Physics* 1981, 75, 5956–5958.
4. Hamm, P.; Lim, M. H.; Hochstrasser, R. M., Structure of the amide I band of peptides measured by femtosecond nonlinear infrared spectroscopy. *Journal of Physical Chemistry B* 1998, 102, 6123–6138.
5. Tanimura, Y.; Mukamel, S., Two-dimensional femtosecond vibrational spectroscopy of liquids. *Journal of Chemical Physics* 1993, 99, 9496–9511.
6. Park, K.; Cho, M., Time- and frequency-resolved coherent two-dimensional IR spectroscopy: Its complementary relationship with the coherent two-dimensional Raman scattering spectroscopy. *Journal of Chemical Physics* 1998, 109, 10559–10569.
7. Hybl, J. D.; Albrecht, A. W.; Gallagher Faeder, S. M.; et al., Two-dimensional electronic spectroscopy. *Chem. Phys. Lett.* 1998, 297, 307–313.
8. Zhao, W.; Wright, J. C., Measurement of $\chi^{(3)}$ for doubly vibrationally enhanced four wave mixing spectroscopy. *Physical Review Letters* 1999, 83, 1950–1953.
9. Brixner, T.; Stenger, J.; Vaswani, H. M.; et al., Two-dimensional spectroscopy of electronic couplings in photosynthesis. *Nature* 2005, 434, 625–628.
10. Cho, M., Coherent two-dimensional optical spectroscopy. *Chemical Reviews* 2008, 108, 1331–1418.
11. Cho, M., Two-dimensional vibrational spectroscopy. In *Advances in multi-photon processes and spectroscopy*, Lin, S. H., Villaeys, A. A., Fujimura, Y., (Eds.) World Scientific Publishing Co.: Singapore, 1999; Vol. 12, pp 229–300.
12. Mukamel, S., Multidimensional femtosecond correlation spectroscopies of electronic and vibrational excitations. *Annual Review of Physical Chemistry* 2000, 51, 691–729.
13. Khalil, M.; Demirdoven, N.; Tokmakoff, A., Coherent 2D IR spectroscopy: Molecular structure and dynamics in solution. *Journal of Physical Chemistry A* 2003, 107, 5258–5279.
14. Woutersen, S.; Hamm, P., Nonlinear two-dimensional vibrational spectroscopy of peptides. *Journal of Physics-Condensed Matter* 2002, 14, R1035–R1062.
15. Jonas, D. M., Two-dimensional femtosecond spectroscopy. *Annual Review of Physical Chemistry* 2003, 54, 425–463.

16. Cho, M., Ultrafast vibrational spectroscopy in condensed phases. *PhysChemComm* 2002, 40–58.
17. Ge, N. H.; Hochstrasser, R. M., Femtosecond two-dimensional infrared spectroscopy: IR-COSY and THIRSTY. *PhysChemComm* 2002, 17–26.
18. Cho, M., Coherent two-dimensional optical spectroscopy. *Bull. Kor. Chem. Soc* 2006, 27, 1940–1960.
19. Cho, M.; Brixner, T.; Stiopkin, I.; et al., Two-dimensional electronic spectroscopy of molecular complexes. *Journal of the Chinese Chemical Society* 2006, 53, (1), 15–24.
20. Cho, M., Spectroscopy: Molecular motion pictures. *Nature* 2006, 444, 431.
21. Kolano, C.; Helbing, J.; Kozinski, M.; et al., Watching hydrogen-bond dynamics in a β -turn by transient two-dimensional infrared spectroscopy. *Nature* 2006, 444, 469–472.
22. Cho, M.; Vaswani, H. M.; Brixner, T.; et al., Exciton analysis in 2D electronic spectroscopy. *Journal of Physical Chemistry B* 2005, 109, 10542–10556.
23. Engel, G. S.; Calhoun, T. R.; Read, E. L.; et al., Evidence for wavelike energy transfer through quantum coherence in photosynthetic systems. *Nature* 2007, 446, 782–786.
24. Fleming, G. R.; Cho, M., Chromophore-solvent dynamics. *Annual Review of Physical Chemistry* 1996, 47, 109–134.
25. De Boeij, W. P.; Pshenichnikov, M. S.; Wiersma, D. A., Ultrafast solvation dynamics explored by femtosecond photon echo spectroscopies. *Annual Review of Physical Chemistry* 1998, 49, 99–123.
26. Zimdars, D.; Tokmakoff, A.; Chen, S.; et al., Picosecond infrared vibrational echoes in a liquid and glass using a free electron laser. *Physical Review Letters* 1993, 70, 2718–2721.
27. Tokmakoff, A., Two-dimensional line shapes derived from coherent third-order non-linear spectroscopy. *Journal of Physical Chemistry A*. 2000, 104, 4247–4255.
28. Kwac, K.; Cho, M., Two-color pump-probe spectroscopies of two- and three-level systems: 2-dimensional line shapes and solvation dynamics. *Journal of Physical Chemistry A* 2003, 107, 5903–5912.
29. Park, K.; Cho, M. H.; Hahn, S.; et al., Two-dimensional vibrational spectroscopy. II. Ab initio calculation of the coherent 2D infrared response function of CHCl_3 and comparison with the 2D Raman response function. *Journal of Chemical Physics* 1999, 111, 4131–4139.
30. Zhao, W.; Wright, J. C., Spectral simplification in vibrational spectroscopy using doubly vibrationally enhanced infrared four wave mixing. *Journal of the American Chemical Society* 1999, 121, 10994–10998.
31. Woutersen, S.; Mu, Y.; Stock, G.; et al., Hydrogen-bond lifetime measured by time-resolved 2D-IR spectroscopy: N-methylacetamide in methanol. *Chemical Physics* 2001, 266, 137–147.
32. Kwac, K.; Lee, H.; Cho, M., Non-Gaussian statistics of amide I mode frequency fluctuation of N-methylacetamide in methanol solution: Linear and nonlinear vibrational spectra. *Journal of Chemical Physical* 2004, 120, 1477.
33. Kim, Y. S.; Hochstrasser, R. M., Chemical exchange 2D IR of hydrogen-bond making and breaking. *Proceeding of the National Academy of Sciences of the United States of America* 2005, 102, 11185–11190.
34. Zheng, J.; Kwac, K.; Asbury, J. B.; et al., Ultrafast dynamics of solute-solvent complexation observed at thermal equilibrium in real time. *Science* 2005, 309, 1338–1343.
35. Cowan, M. L.; Bruner, B. D.; Huse, N.; et al., Ultrafast memory loss and energy redistribution in the hydrogen bond network of liquid H_2O . *Nature* 2005, 434, 199–202.

36. Asbury, J. B.; Steinel, T.; Stromberg, C.; et al., Water dynamics: Vibrational echo correlation spectroscopy and comparison to molecular dynamics simulations. *Journal of Physical Chemistry A* 2004, 108, 1107–1119.
37. Eaves, J. D.; Loparo, J. J.; Fecko, C. J.; et al., Hydrogen bonds in liquid water are broken only fleetingly. *Proceeding of the National Academy of Sciences of the United States of America* 2005, 102, 13019–13022.
38. Tian, P.; Keusters, D.; Suzuki, Y.; et al., Femtosecond phase-coherent two-dimensional spectroscopy. *Science* 2003, 300, 1553–1555.
39. DeCamp, M. F.; DeFlores, L. P.; Jones, K. C.; et al., Single-shot two-dimensional infrared spectroscopy. *Optics Express* 2007, 15, 233–241.
40. DeCamp, M. F.; Tokmakoff, A., Single-shot two-dimensional spectrometer. *Optics Letters* 2006, 31, 113–115.

2 Quantum Dynamics

A principal goal of spectroscopic investigation is to study electronic or magnetic properties of materials by measuring radiation–matter interaction-induced changes of radiation states in frequency and/or time domains.^{1–4} Since the electromagnetic field amplitude oscillates and the temporal envelope of laser pulse used changes in time,⁵ the radiation–matter interaction Hamiltonian is intrinsically time-dependent, and the time evolutions of the matter states might be fully determined by the time-dependent Schrödinger equation,

$$\frac{\partial}{\partial t} |\psi(t)\rangle = -\frac{i}{\hbar} \hat{H}(t) |\psi(t)\rangle \quad (2.1)$$

Here, $|\psi(t)\rangle$ is the Dirac *ket* state. The corresponding *bra* state is denoted as $\langle\psi(t)|$. The time-dependent Schrödinger equation (2.1) is one of the most fundamental and important postulates in quantum mechanics.^{6–8} In this chapter, we introduce the concept of linear vector (wavefunction) and matrix (density operator) spaces to describe the quantum dynamics of matters interacting with external radiations.

2.1 TIME EVOLUTION IN HILBERT SPACE

Hilbert space is a linear vector space of functions. In quantum mechanics, a vector in the Hilbert space is wavefunction $\psi(t)$ and the complete and orthonormal basis set used to define the quantum mechanical Hilbert space consists of eigenvectors of the time-independent Schrödinger equation, that is,

$$\hat{H} |\phi_n\rangle = E_n |\phi_n\rangle. \quad (2.2)$$

From the orthonormalization condition of unit vectors in the Hilbert space, we have

$$\langle\phi_n|\phi_m\rangle = \delta_{nm}. \quad (2.3)$$

From the completeness condition, the identity operator is defined as

$$\sum_m |\phi_m\rangle\langle\phi_m| = 1. \quad (2.4)$$

With the Dirac's bra-ket notation, the inner product of any given pair of vectors (wavefunctions) is defined as

$$\langle\psi_j(t)|\psi_k(t)\rangle \equiv \int_V \psi_j^*(\mathbf{r},t)\psi_k(\mathbf{r},t) d\mathbf{r}, \quad (2.5)$$

where V is the quantization volume.

Any vector, wavefunction in this Hilbert space can therefore be expanded as

$$|\psi(t)\rangle = \sum_n c_n(t) |\phi_n\rangle \quad (2.6)$$

where the expansion coefficient is the projection of the vector onto each unit vector,

$$c_n(t) \equiv \langle \phi_n | \psi(t) \rangle. \quad (2.7)$$

EXERCISE 2.1

Consider a two-level system. Assume that the system at time t_0 is a superposition state of the two eigenvectors, that is, $|\psi(t_0)\rangle = \frac{1}{\sqrt{2}}(|\phi_1\rangle + |\phi_2\rangle)$, and that the Hamiltonian is given as $\hat{H} = \Delta(|\phi_1\rangle\langle\phi_2| + |\phi_2\rangle\langle\phi_1|)$. Calculate the ket function $|\psi(t)\rangle$ at time t .

In the case when the Hamiltonian is time-independent, the formal solution of the time-dependent Schrödinger equation is given as

$$|\psi(t)\rangle = \exp\left(-\frac{i}{\hbar}\hat{H}(t-t_0)\right)|\psi(t_0)\rangle = u(t, t_0)|\psi(t_0)\rangle \quad (2.8)$$

where $u(t, t_0)$ represents the forward time evolution operator when $t > t_0$:

$$u(t, t_0) \equiv \exp\left(-\frac{i}{\hbar}\hat{H}(t-t_0)\right). \quad (2.9)$$

The backward time evolution operator is then defined as

$$u^\dagger(t, t_0) \equiv \exp\left(\frac{i}{\hbar}\hat{H}(t-t_0)\right). \quad (2.10)$$

It is noted that the Hamiltonian operator is Hermitian. The time evolution operator $u(t, t_0)$ ($u^\dagger(t, t_0)$) describes the forward (backward) time evolution of the ket (bra) vector, whereas the same operator does backward (forward) time evolution of the bra (ket) vector. The Hilbert space for a ket vector is nothing but a mirror image of that for a bra vector. The two spaces are related to each other via Hermitian conjugate relationship. Note that the quantum mechanical Hilbert space is a complex space where a vector can have both real and imaginary parts. If one needs to calculate any real observable at time t , one should consider the ket and bra vectors at t simultaneously. However, since the time evolution of the ket vector is just a mirror image of (Hermitian conjugate relationship to) that of the corresponding bra vector, it is enough to consider one of the two time-evolved vectors in a given Hilbert space.

EXERCISE 2.2

Prove that $u(t, t_0)u^\dagger(t, t_0) = u^\dagger(t, t_0)u(t, t_0) = 1$. (Hint: use $\exp(x) = 1 + \sum_n (1/n!)x^n$ and the Baker-Hausdorff lemma, $e^{\hat{A}}e^{\hat{B}} = e^{\hat{A}+\hat{B}}e^{(1/2)[\hat{A}, \hat{B}]}$.)⁹

In the Schrödinger picture, where the wavefunction is time-dependent whereas an operator \hat{A} corresponding to the observable A is not, the expectation value may be calculated as, on the basis of one of the quantum mechanical postulates,

$$\bar{A}(t) = \langle \psi(t) | \hat{A} | \psi(t) \rangle = \langle \psi(t_0) | u^\dagger(t, t_0) \hat{A} u(t, t_0) | \psi(t_0) \rangle. \quad (2.11)$$

The physical meaning of the right-hand side of Equation 2.11 is that when the initial wavefunction is known at time t_0 , the ket vector $|\psi(t_0)\rangle$ evolves in the forward direction in time from t_0 to t by the $u(t, t_0)$ operator, and the bra vector $\langle \psi(t_0)|$ also does from t_0 to t by the $u^\dagger(t, t_0)$ operator. Then, the expectation value of \hat{A} over the wavefunction at time t provides the value of $\bar{A}(t)$.

Defining the time-dependent operator $\hat{A}(t)$ as

$$\hat{A}_H(t) = u^\dagger(t, t_0) \hat{A} u(t, t_0) = \exp\left(\frac{i}{\hbar} \hat{H}(t - t_0)\right) \hat{A} \exp\left(-\frac{i}{\hbar} \hat{H}(t - t_0)\right), \quad (2.12)$$

the expectation value of \hat{A} at time t can be rewritten as

$$\bar{A}(t) = \langle \psi(t_0) | \hat{A}_H(t) | \psi(t_0) \rangle. \quad (2.13)$$

This route to the calculation of any expectation value has been known to be the Heisenberg picture.

EXERCISE 2.3

Show that the time-dependent operator defined in Equation 2.12 obeys the Heisenberg equation, i.e., $\frac{\partial}{\partial t} \hat{A}_H(t) = \frac{i}{\hbar} [\hat{H}, \hat{A}_H(t)]$. Here, it is assumed that the operator \hat{A} does not depend on time explicitly.

In spectroscopy, the radiation–matter interaction Hamiltonian is time-dependent so that the time evolution of the wavefunction needs to be described differently from the case of time-independent Hamiltonian. The total Hamiltonian of the composite system consisting of matter and radiation may be written as

$$\hat{H}(t) = \hat{H}_{mat} + \hat{H}_{rad} + \hat{H}_{rad-mat}(t). \quad (2.14)$$

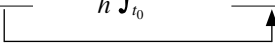
From the time-dependent Schrödinger equation (2.1), let us assume that the formal solution of the wavefunction of the ket vector is given as

$$|\psi(t)\rangle = U(t, t_0) |\psi(t_0)\rangle. \quad (2.15)$$

To determine the time evolution operator, $U(t, t_0)$, in Equation 2.15, one can substitute Equation 2.15 into 2.1 and find that

$$\frac{\partial}{\partial t} U(t, t_0) = -\frac{i}{\hbar} \hat{H}(t) U(t, t_0). \quad (2.16)$$

Carrying out the integration of Equation 2.16 with respect to t , we have

$$U(t, t_0) = 1 - \frac{i}{\hbar} \int_{t_0}^t d\tau \hat{H}(\tau) U(\tau, t_0). \quad (2.17)$$


By repeatedly inserting the right-hand side of Equation 2.17 into the $U(\tau, t_0)$ term in the integrand, one can formally derive the following series solution for the time evolution operator, $U(t, t_0)$, when the Hamiltonian is explicitly time-dependent, as

$$U(t, t_0) = 1 + \sum_{n=1}^{\infty} \left(-\frac{i}{\hbar} \right)^n \int_{t_0}^t d\tau_n \int_{t_0}^{\tau_n} d\tau_{n-1} \cdots \int_{t_0}^{\tau_2} d\tau_1 \hat{H}(\tau_n) \hat{H}(\tau_{n-1}) \cdots \hat{H}(\tau_1). \quad (2.18)$$

Note that the above series expansion is not identical to the Taylor expansion of the exponential function and that the integration time variables have the following order, $\tau_n \geq \tau_{n-1} \geq \cdots \geq \tau_1$. For the sake of notational simplicity of the forward time evolution operator $U(t, t_0)$, the positive time-ordering exponential operator is defined as

$$U(t, t_0) = \exp_+ \left(-\frac{i}{\hbar} \int_{t_0}^t d\tau \hat{H}(\tau) \right). \quad (2.19)$$

EXERCISE 2.4

Show that the forward time evolution operator $U(t, t_0)$ defined in Equation 2.19 with 2.18 becomes $u(t, t_0)$ when the Hamiltonian is time-independent.

Then, the backward time evolution operator, which is the Hermitian conjugate of $U(t, t_0)$, is found to be

$$\begin{aligned} U^\dagger(t, t_0) &= \exp_- \left(\frac{i}{\hbar} \int_{t_0}^t d\tau \hat{H}(\tau) \right) \\ &= 1 + \sum_{n=1}^{\infty} \left(\frac{i}{\hbar} \right)^n \int_{t_0}^t d\tau_n \int_{t_0}^{\tau_n} d\tau_{n-1} \cdots \int_{t_0}^{\tau_2} d\tau_1 \hat{H}(\tau_1) \hat{H}(\tau_2) \cdots \hat{H}(\tau_n). \end{aligned} \quad (2.20)$$

EXERCISE 2.5

Show that $U(t, t_0)U^\dagger(t, t_0) = U^\dagger(t, t_0)U(t, t_0) = 1$.

2.2 TIME-DEPENDENT PERTURBATION THEORY IN HILBERT SPACE

Although the time evolution operators in Equations 2.18 and 2.20 are exact for describing the quantum dynamics of composite system consisting of materials, bath, and radiation, the corresponding time-dependent Schrödinger equation cannot be directly

solved to calculate any expectation values, quantum transition amplitudes and probabilities, and matter's electronic and magnetic properties. That is not only because the series summation requires an infinite number of terms but also because the eigenvalue equation such as $\hat{H}(\tau_1)|\psi\rangle = E|\psi\rangle$ cannot be easily solved for the Hamiltonian describing optical chromophores interacting with both surrounding bath degrees of freedom and external radiations. Therefore, it is inevitable to develop a proper time-dependent perturbation theory, and the total Hamiltonian is divided into two parts as

$$\hat{H}(t) = \hat{H}_0(t) + \hat{H}'(t), \quad (2.21)$$

where the zero-order Hamiltonian $\hat{H}_0(t)$ serves as the reference and the second term $\hat{H}'(t)$ is treated as perturbation Hamiltonian. In spectroscopy, the system, bath, and radiation Hamiltonians constitute the zero-order Hamiltonian, and the field-matter interaction is considered to be the perturbation Hamiltonian. The perturbation theory can thus provide quantitatively reliable information when $\hat{H}'(t)$ is properly chosen so that the perturbation series successfully converges.

It turns out that the interaction picture instead of the Schrödinger or Heisenberg picture discussed above is quite useful for a development of time-dependent perturbation theory. In the interaction picture, the time evolutions of the wavefunction is fully described by the zero-order Hamiltonian $\hat{H}_0(t)$, not by the total Hamiltonian $\hat{H}(t)$. In addition, the perturbation Hamiltonian $\hat{H}'(t)$ also evolves in time in the Heisenberg picture determined by $\hat{H}_0(t)$. Thus, the interaction picture can be viewed as a hybrid of both Schrödinger and Heisenberg pictures. We assume that the forward time evolution operator $U(t, t_0)$ can be written as a product of two operators as

$$U(t, t_0) = U_0(t, t_0)U_I(t, t_0), \quad (2.22)$$

where

$$U_0(t, t_0) = \exp_+ \left(-\frac{i}{\hbar} \int_{t_0}^t d\tau \hat{H}_0(\tau) \right) \quad (2.23)$$

$$U_I(t, t_0) = \exp_+ \left(-\frac{i}{\hbar} \int_{t_0}^t d\tau \hat{H}'_I(\tau) \right). \quad (2.24)$$

Here, the time-dependent perturbation Hamiltonian operator in the Heisenberg picture described by the zero-order Hamiltonian, $\hat{H}'_0(t)$, is defined as

$$\hat{H}'_I(t) = U_0^\dagger(t, t_0) \hat{H}'(t) U_0(t, t_0). \quad (2.25)$$

In this interaction picture, the expectation value of the time-dependent operator $\hat{A}(t)$ is given as

$$\begin{aligned} \bar{A}(t) &= \langle \psi(t_0) | U_I^\dagger(t, t_0) U_0^\dagger(t, t_0) \hat{A}(t) U_0(t, t_0) U_I(t, t_0) | \psi(t_0) \rangle \\ &= \langle \psi_I(t) | \hat{A}_I(t) | \psi_I(t) \rangle, \end{aligned} \quad (2.26)$$

where

$$\hat{A}_I(t) \equiv U_0^\dagger(t, t_0) \hat{A}(t) U_0(t, t_0). \quad (2.27)$$

$$|\psi_I(t)\rangle \equiv U_I(t, t_0) |\psi(t_0)\rangle. \quad (2.28)$$

Note that, in the interaction picture, both the wavefunction and operator evolve in time.

EXERCISE 2.6

Show that $|\psi(t)\rangle = U_0(t, t_0) U_I(t, t_0) |\psi(t_0)\rangle$ indeed obeys the time-dependent Schrödinger equation.

In order to develop a time-dependent perturbation theory, one can expand $U_I(t, t_0)$ given in Equation 2.24 as a power series of the time-evolved perturbation Hamiltonian $\hat{H}'_I(\tau)$ and find that the forward time evolution operator can be expanded as

$$\begin{aligned} U(t, t_0) &= U_0(t, t_0) + \left(-\frac{i}{\hbar}\right) \int_{t_0}^t d\tau_1 U_0(t, \tau_1) \hat{H}'(\tau_1) U_0(\tau_1, t_0) \\ &\quad + \left(-\frac{i}{\hbar}\right)^2 \int_{t_0}^t d\tau_2 \int_{t_0}^{\tau_2} d\tau_1 U_0(t, \tau_2) \hat{H}'(\tau_2) U_0(\tau_2, \tau_1) \hat{H}'(\tau_1) U_0(\tau_1, t_0) + \dots \\ &= \sum_{n=0}^{\infty} U_n(t, t_0), \end{aligned} \quad (2.29)$$

where the n th-order perturbation term, $U_n(t, t_0)$, is defined as

$$\begin{aligned} U_n(t, t_0) &\equiv \left(-\frac{i}{\hbar}\right)^n \int_{t_0}^t d\tau_n \int_{t_0}^{\tau_n} d\tau_{n-1} \dots \int_{t_0}^{\tau_2} d\tau_1 U_0(t, \tau_n) \hat{H}'(\tau_n) U_0(\tau_n, \tau_{n-1}) \times \dots \\ &\quad \times U_0(\tau_2, \tau_1) \hat{H}'(\tau_1) U_0(\tau_1, t_0). \end{aligned} \quad (2.30)$$

Similarly, the backward time evolution operator in the interaction picture can be written as

$$U^\dagger(t, t_0) = U_I^\dagger(t, t_0) U_0^\dagger(t, t_0) = \sum_{n=0}^{\infty} U_n^\dagger(t, t_0) \quad (2.31)$$

where

$$\begin{aligned} U_n^\dagger(t, t_0) &\equiv \left(\frac{i}{\hbar}\right)^n \int_{t_0}^t d\tau_n \int_{t_0}^{\tau_n} d\tau_{n-1} \dots \int_{t_0}^{\tau_2} d\tau_1 U_0^\dagger(\tau_1, t_0) \hat{H}'(\tau_1) U_0^\dagger(\tau_2, \tau_1) \times \dots \\ &\quad \times U_0^\dagger(\tau_n, \tau_{n-1}) \hat{H}'(\tau_n) U_0^\dagger(t, \tau_n). \end{aligned} \quad (2.32)$$

EXERCISE 2.7

To obtain Equations 2.30 and 2.32, the following operator equalities, $U_0(t, t_0)U_0^\dagger(\tau, t_0) = U_0(t, \tau)$ and $U_0(\tau, t_0)U_0^\dagger(t, t_0) = U_0^\dagger(t, \tau)$, were used. Prove these two equalities.

2.3 DIAGRAM REPRESENTATION OF THE TIME-DEPENDENT PERTURBATION THEORY IN HILBERT SPACE

Formal expressions and results on the time evolution operators and expectation values in terms of perturbation series were presented and discussed above, but it has always been found to be useful to represent each term in terms of graphical diagrams. In this regard, the Feynman diagram representation of the perturbation theory has been considered to be one of the simplest pictures and allows one to understand the time evolution of the system when a certain number of perturbation actions to the zero-order wavefunction occur in time. Here, we will introduce a modified Feynman diagram technique for the perturbation theory. The complete time evolution operator $U(t, t_0)$ was given as a series of perturbation terms as

$$U(t, t_0) = U_0(t, t_0) + U_1(t, t_0) + U_2(t, t_0) + \dots \tag{2.33}$$

It will be assumed that the diagrams corresponding to each term in Equation 2.33 are defined as

$$\leftarrow = \leftarrow + \leftarrow \overset{\xi}{\tau_1} + \leftarrow \overset{\xi}{\tau_2} \overset{\xi}{\tau_1} + \dots \tag{2.34}$$

The thick, solid arrow pointing from right to left represents the total time evolution operator $U(t, t_0)$, whereas the thin arrow represents the zero-order time evolution operator, $U_0(\tau, t_0)$, which is determined by the zero-order Hamiltonian $\hat{H}_0(t)$. The wavy line symbol ξ in the Feynman diagrammatic representation of $U_1(t, t_0)$ corresponds to the action of the perturbation Hamiltonian at τ_1 . Note that the first-order term, $U_1(t, t_0)$, describes the time evolution of the wavefunction from t_0 to t when there is a single perturbation by $\hat{H}'(\tau_1)$ at time τ_1 ($t \geq \tau_1 \geq t_0$). Since the perturbation action occurs at any time from t_0 to t , one should take into consideration all possibilities so that the integration over τ_1 in the range from t_0 to t should be performed. From Equation 2.15, the first time-derivative of \leftarrow is given as

$$\frac{\partial}{\partial t} \leftarrow = -\frac{i}{\hbar} \hat{H}(t) \leftarrow \tag{2.35}$$

Similarly, the backward time evolution operator given as a series of the perturbation terms is

$$U^\dagger(t, t_0) = U_0^\dagger(t, t_0) + U_1^\dagger(t, t_0) + U_2^\dagger(t, t_0) + \dots \tag{2.36}$$

and the corresponding diagram representation is

$$\rightarrow = \rightarrow + \overset{\xi}{\tau_1} \rightarrow + \overset{\xi}{\tau_1} \overset{\xi}{\tau_2} \rightarrow + \dots \tag{2.37}$$

Note that the directions of the arrows are the opposite of those in the forward time evolution operators, indicating that the time runs from left to right. The first derivative of \longrightarrow satisfies the following differential equation:

$$\frac{\partial}{\partial t} \longrightarrow = \longrightarrow \frac{i}{\hbar} \hat{H}(t). \quad (2.38)$$

Using the diagrams introduced above, the time-evolved ket and bra vectors can be diagrammatically represented as

$$|\psi(t)\rangle = \longleftarrow |\psi(t_0)\rangle + \longleftarrow \xi |\psi(t_0)\rangle + \longleftarrow \xi \xi |\psi(t_0)\rangle + \dots \quad (2.39)$$

$$\langle \psi(t) | = \langle \psi(t_0) | \longrightarrow + \langle \psi(t_0) | \xrightarrow{\xi} + \langle \psi(t_0) | \xrightarrow{\xi \xi} + \dots \quad (2.40)$$

Therefore, the expectation value of an operator $\hat{A}(t)$ is, in the diagram representation, simply given as

$$\bar{A}(t) = \langle \psi(t_0) | \longrightarrow \hat{A}(t) \longleftarrow | \psi(t_0) \rangle. \quad (2.41)$$

Then, the series expansion of $\bar{A}(t)$ is

$$\bar{A}(t) = \sum_{n=0}^{\infty} \bar{A}^{(n)}(t), \quad (2.42)$$

where the first three perturbation expansion terms are

$$\begin{aligned} \bar{A}^{(0)}(t) &= \langle \psi(t_0) | \longrightarrow \hat{A} \longleftarrow | \psi(t_0) \rangle \\ \bar{A}^{(1)}(t) &= \langle \psi(t_0) | \longrightarrow \hat{A} \xrightarrow{\xi} | \psi(t_0) \rangle + \langle \psi(t_0) | \xrightarrow{\xi} \hat{A} \longleftarrow | \psi(t_0) \rangle \\ \bar{A}^{(2)}(t) &= \langle \psi(t_0) | \longrightarrow \hat{A} \xrightarrow{\xi \xi} | \psi(t_0) \rangle + \langle \psi(t_0) | \xrightarrow{\xi} \hat{A} \xrightarrow{\xi} | \psi(t_0) \rangle + \langle \psi(t_0) | \longrightarrow \hat{A} \xrightarrow{\xi \xi} | \psi(t_0) \rangle. \end{aligned} \quad (2.43)$$

Instead of considering the perturbation expansion of the wavefunction, one can equally calculate the same expectation value in the Heisenberg picture as

$$\bar{A}(t) = \langle \psi(t_0) | \hat{A}_H(t) | \psi(t_0) \rangle = \langle \psi(t_0) | \sum_{n=0}^{\infty} \hat{A}_H^{(n)}(t) | \psi(t_0) \rangle \quad (2.44)$$

where, in the diagram representation, the perturbationally expanded time-evolved Heisenberg operators of $\hat{A}(t)$ are

$$\begin{aligned}
 \hat{A}_H(t) &= \text{---} \hat{A}(t) \text{---} \\
 \hat{A}_H^{(0)}(t) &= \text{---} \hat{A}(t) \text{---} \\
 \hat{A}_H^{(1)}(t) &= \overset{\xi}{\text{---}} \hat{A}(t) \text{---} + \text{---} \hat{A}(t) \overset{\xi}{\text{---}} \\
 \hat{A}_H^{(2)}(t) &= \overset{\xi \xi}{\text{---}} \hat{A}(t) \text{---} + \overset{\xi}{\text{---}} \hat{A}(t) \overset{\xi}{\text{---}} + \text{---} \hat{A}(t) \overset{\xi \xi}{\text{---}} \quad (2.45)
 \end{aligned}$$

EXERCISE 2.8

Show that $\hat{A}_H(t)$ defined in Equation 2.45 is identical to $U^\dagger(t, t_0)\hat{A}U(t, t_0)$ and that its time evolution is determined by the Heisenberg equation (see Exercise 2.3).

2.4 TRANSITION AMPLITUDE AND PROBABILITY IN HILBERT SPACE

Most of spectroscopic observables require calculations of the amplitude or probability of the transition from a specific initial state $|m\rangle$ at t_0 to a final state $|n\rangle$ at a later time t , when such a transition is induced by the perturbation Hamiltonian $\hat{H}'(t)$. By definition, the transition amplitude in this case is calculated by

$$TA_{nm}(t) \equiv \langle n | U(t, t_0) | m \rangle = \langle n | U_0(t, t_0) U_I(t, t_0) | m \rangle. \quad (2.46)$$

We shall assume that the initial and final states are eigenvectors (stationary states) of the zero-order Hamiltonian, i.e., $H_0 |m\rangle = E_m |m\rangle$ and $H_0 |n\rangle = E_n |n\rangle$. Then, the first-order perturbation theory provides us the first-order transition amplitude as

$$TA_{nm}^{(1)}(t) \equiv \langle n | U_I(t, t_0) | m \rangle = \left(-\frac{i}{\hbar} \right) \int_{t_0}^t d\tau_1 \langle n | U_0(t, \tau_1) \hat{H}'(\tau_1) U_0(\tau_1, t_0) | m \rangle. \quad (2.47)$$

This can be re-expressed as, in terms of the corresponding Feynman diagram,

$$TA_{nm}^{(1)}(t) = \langle n | \overset{\xi}{\text{---}} | m \rangle. \quad (2.48)$$

However, what is experimentally measured is not the transition amplitude but the corresponding transition probability that is defined as the square of the transition amplitude as

$$TP_{nm}(t) \equiv |TA_{nm}(t)|^2. \quad (2.49)$$

We find that the second-order transition probability of being in state $|n\rangle$ at time t is

$$TP_{nm}^{(2)}(t) = \langle n | \overleftarrow{\xi} | m \rangle \langle m | \overrightarrow{\xi} | n \rangle. \quad (2.50)$$

This expression can be written as a double integral as

$$\begin{aligned} TP_{nm}^{(2)}(t) = & \left(\frac{1}{\hbar^2} \right) \int_{t_0}^t d\tau_1 \int_{t_0}^t d\tau_2 \langle n | U_0(t, \tau_1) \hat{H}'(\tau_1) U_0(\tau_1, t_0) | m \rangle \\ & \times \langle m | U_0^\dagger(\tau_2, t_0) \hat{H}'(\tau_2) U_0^\dagger(t, \tau_2) | n \rangle. \end{aligned} \quad (2.51)$$

For the sake of simplicity, let us consider the case that the zero-order Hamiltonian does not explicitly depend on time. Then, Equation 2.51 can be simplified as

$$TP_{nm}^{(2)}(t) = \frac{1}{\hbar^2} \left| \int_{t_0}^t d\tau e^{i\omega_{nm}\tau} H'_{nm}(\tau) \right|^2 \quad (2.52)$$

where $\omega_m \equiv E_m/\hbar$, $\omega_{nm} \equiv \omega_n - \omega_m$, and

$$H'_{nm}(\tau) \equiv \langle n | \hat{H}'(\tau) | m \rangle. \quad (2.53)$$

If the initial time t_0 is $-\infty$, the transition probability evaluated at $t = \infty$ is

$$TP_{nm}^{(2)}(t = \infty) = \frac{1}{\hbar^2} |\tilde{H}'_{nm}(\omega_{nm})|^2 \quad (2.54)$$

where $\tilde{H}'_{nm}(\omega_{nm})$ is the Fourier transform of $H'_{nm}(t)$ at $\omega = \omega_{nm}$. Throughout this book, the Fourier and inverse Fourier transforms are defined as

$$\tilde{f}(\omega) = \int_{-\infty}^{\infty} dt f(t) e^{i\omega t} \quad (2.55)$$

$$f(t) = \frac{1}{2\pi} \int_{-\infty}^{\infty} dt \tilde{f}(\omega) e^{-i\omega t}. \quad (2.56)$$

EXERCISE 2.9

One can derive the well-known Fermi's Golden Rule (FGR) expression for a rate of transition, $w = \frac{2\pi}{\hbar} \rho(E_n) |H'_{nm}|^2$, where the perturbation Hamiltonian is time-independent so that H'_{nm} is a constant. To obtain the FGR expression given above, it was assumed (1) that the final states are closely spaced in energy so that they form a continuum with density of states $\rho(E_n)$, (2) that only the long-time behavior is considered, (3) that H'_{nm} and $\rho(E_n)$ do not strongly depend on n , and (4) that the above second-order expression for $TP_{nm}^{(2)}(t)$ is valid.

In order to obtain the result in Equation 2.54, it was assumed that the initial state at t_0 is a pure state on $|m\rangle$. However, if the initial state is a mixed state such as a canonical ensemble, one should take an ensemble average over the thermal distribution of the initial states. Suppose that the probability of being in state $|m\rangle$ is $P_m(T)$ at temperature T . Then, the transition probability of finding the system being in state $|n\rangle$ is given by a sum over all $|m\rangle$ with distribution $P_m(T)$ as

$$\begin{aligned} TP_n^{(2)}(t) &= \sum_m P_m(T) \times TP_{nm}^{(2)}(t) \\ &= \sum_m \langle n | \overleftarrow{\xi} | m \rangle P_m(T) \langle m | \overrightarrow{\xi} | n \rangle. \end{aligned} \quad (2.57)$$

If one introduces an operator $\rho(t_0)$ in a matrix form and if the diagonal matrix elements, which are still operator, are given as $\rho_{mm}(t_0) = |m\rangle P_m(T) \langle m|$, the transition probability in Equation 2.57 can be rewritten as

$$\begin{aligned} TP_n^{(2)}(t) &= \sum_m \langle n | \overleftarrow{\xi} \rho_{mm}(t_0) \overrightarrow{\xi} | n \rangle \\ &= \langle n | \overleftarrow{\xi} \text{Tr}[\rho(t_0)] \overrightarrow{\xi} | n \rangle. \end{aligned} \quad (2.58)$$

Now, the second-order time-evolved density operator $\rho^{(2)}(t)$ is graphically represented as

$$\rho^{(2)}(t) = \overleftarrow{\xi} \text{Tr}[\rho(t_0)] \overrightarrow{\xi} \quad (2.59)$$

so that we have

$$TP_n^{(2)}(t) = \rho_{nn}^{(2)}(t) \equiv \langle n | \rho^{(2)}(t) | n \rangle. \quad (2.60)$$

Using the description of the time evolution of wavefunction in Hilbert space in terms of the time evolution operators, one can calculate the transition amplitude but not probability directly. As shown above from Equations 2.57 to 2.60, the transition probability calculation requires a few more steps of derivations and additional ensemble averaging calculation when the system is initially in a thermal equilibrium state at finite temperature T . However, by directly considering the time evolution operator in a matrix form instead of a vectorial form, one can easily perform such multistep calculations. In addition, an ensemble averaging calculation is straightforward since the initial density operator contains information on the mixed state. Furthermore, for developing a higher-order time-dependent perturbation theory, the density operator representation has been found to be useful for bookkeeping quite a number of nonlinear optical transition pathways contributing to the transition probability or measured signal of interest.

2.5 TIME EVOLUTION IN LIOUVILLE SPACE

In the Hilbert space spanned by the eigenvectors of the time-independent Schrodinger equation, wavefunction is a vector and its time evolution is determined by the time-dependent Schrodinger equation. However, if one has to deal with a statistically mixed state such as systems in a canonical ensemble, transition probability calculation is often easier and conceptually simpler if the dynamics of the system are described in a Liouville (density matrix) space.^{2, 10, 11} In addition, time evolutions of quantum coherence and population can be easily described by using the density operator formalism.¹² In the previous section, it was already shown that the second-order perturbation theory for calculating transition probability can be expressed in terms of density operator.

The conventional definition of density operator is

$$\rho(t) = |\psi(t)\rangle\langle\psi(t)|. \quad (2.61)$$

Using the diagrammatic representations of the forward and backward time evolution operators $U(t, t_0)$ and $U^\dagger(t, t_0)$, one can re-express Equation 2.61 as

$$\rho(t) = \leftarrow \rho(t_0) \rightarrow \quad (2.62)$$

with $\rho(t_0) = |\psi(t_0)\rangle\langle\psi(t_0)|$. In comparison to the Hilbert space where wavefunction is a linear vector, the corresponding vector in Liouville space is density operator. One can prove that the density operator defined above obeys the following differential equation:

$$\frac{\partial}{\partial t} \rho(t) = -\frac{i}{\hbar} [\hat{H}(t), \rho(t)], \quad (2.63)$$

which is the quantum Liouville equation. Equation 2.63 can be obtained by using Equations 2.35 and 2.38 and taking the first derivative of Equation 2.62, that is,

$$\frac{\partial}{\partial t} \rho(t) = \left(\frac{\partial}{\partial t} \leftarrow \right) \rho(t_0) \rightarrow + \leftarrow \rho(t_0) \left(\frac{\partial}{\partial t} \rightarrow \right). \quad (2.64)$$

We now search for a simple diagrammatic representation of the time evolution operator in the Liouville space. In the case of the time evolution of a wavefunction in a Hilbert space, a single arrow \leftarrow was enough, since the time evolution of either ket or bra vector is all we need. On the other hand, since the density operator is a product of ket and bra vectors, one should take into consideration of time evolutions of ket and bra sides altogether. Therefore, we introduce another type of arrow representing the time evolution of the density operator as

$$\rho(t) = \leftarrow \rho(t_0) \rightarrow \quad (2.65)$$

Introducing the Liouville operator, L , defined as

$$L(t)\hat{A}(t) = [\hat{H}(t), \hat{A}(t)], \quad (2.66)$$

the quantum Liouville equation in 2.63 can be rewritten as

$$\frac{\partial}{\partial t} \rho(t) = -\frac{i}{\hbar} L(t) \rho(t). \quad (2.67)$$

Then, one can find that the time evolution operator in the Liouville space is given as

$$V(t, t_0) = \exp_+ \left(-\frac{i}{\hbar} \int_{t_0}^t d\tau L(\tau) \right), \quad (2.68)$$

which corresponds to \Leftarrow , that is,

$$V(t, t_0) = \Leftarrow. \quad (2.69)$$

The Hermitian conjugate of $V(t, t_0)$ is then

$$V^\dagger(t, t_0) = \exp_- \left(\frac{i}{\hbar} \int_{t_0}^t d\tau L(\tau) \right) \quad (2.70)$$

so that we have

$$V^\dagger(t, t_0) = \Rightarrow. \quad (2.71)$$

Now, from the definition of the expectation value in Equation 2.41 and using the completeness condition in Equation 2.3, we can rewrite the expectation value as

$$\begin{aligned} \bar{A}(t) &= \sum_{m,n} \langle \psi(t_0) | \Rightarrow | m \rangle A_{mn}(t) \langle n | \Leftarrow | \psi(t_0) \rangle. \\ &= \sum_{m,n} A_{mn}(t) \langle n | \Leftarrow | \psi(t_0) \rangle \langle \psi(t_0) | \Rightarrow | m \rangle \\ &= \sum_{m,n} A_{mn}(t) \rho_{nm}(t) \\ &= Tr[\hat{A}(t) \rho(t)] \\ &= \langle \hat{A}(t) \rho(t) \rangle. \end{aligned} \quad (2.72)$$

Here, the angle bracket $\langle \hat{O} \rangle$ without bra-ket notation means taking the trace of \hat{O} in matrix representation. Using the diagrammatic technique, the expectation value can be simply represented as

$$\bar{A}(t) = \langle \hat{A}(t) \Leftarrow \rho(t_0) \rangle. \quad (2.73)$$

2.6 TIME-DEPENDENT PERTURBATION THEORY IN LIOUVILLE SPACE

When the total Hamiltonian is divided into the zero-order reference Hamiltonian and the perturbation Hamiltonian as Equation 2.21, the Liouville operator can also be written as

$$L(t) = L_0(t) + L'(t). \quad (2.74)$$

Then, in the interaction representation, the time evolution operator in the Liouville space is found to be

$$V(t, t_0) = V_0(t, t_0)V_I(t, t_0) \quad (2.75)$$

where

$$V_0(t, t_0) = \exp_+ \left(-\frac{i}{\hbar} \int_{t_0}^t d\tau L_0(\tau) \right) \quad (2.76)$$

$$V_I(t, t_0) = \exp_+ \left(-\frac{i}{\hbar} \int_{t_0}^t d\tau L'_I(\tau) \right). \quad (2.77)$$

Here, the time-dependent operator $L'_I(t)$ in the interaction representation is defined as

$$L'_I(t) = V_0^\dagger(t, t_0)L'(t)V_0(t, t_0). \quad (2.78)$$

Following the same procedure used to derive the time-ordered expansion expression for $U(t, t_0)$ with respect to $H'(t)$, one can expand the Liouville space time-evolution operator $V(t, t_0)$ as

$$\begin{aligned} V(t, t_0) &= V_0(t, t_0) + \left(-\frac{i}{\hbar} \right) \int_{t_0}^t d\tau_1 V_0(t, \tau_1) L'(\tau_1) V_0(\tau_1, t_0) \\ &\quad + \left(-\frac{i}{\hbar} \right)^2 \int_{t_0}^t d\tau_2 \int_{t_0}^{\tau_2} d\tau_1 V_0(t, \tau_2) L'(\tau_2) V_0(\tau_2, \tau_1) L'(\tau_1) V_0(\tau_1, t_0) + \dots \\ &= \sum_{n=0}^{\infty} V_n(t, t_0), \end{aligned} \quad (2.79)$$

where the n th-order perturbation expansion term, $V_n(t, t_0)$, is defined as

$$V_n(t, t_0) \equiv \left(-\frac{i}{\hbar}\right)^n \int_{t_0}^t d\tau_n \int_{t_0}^{\tau_n} d\tau_{n-1} \cdots \int_{t_0}^{\tau_2} d\tau_1 V_0(t, \tau_n) L'(\tau_n) V_0(\tau_n, \tau_{n-1}) \times \cdots \\ \times V_0(\tau_2, \tau_1) L'(\tau_1) V_0(\tau_1, t_0). \tag{2.80}$$

Similarly, the backward time evolution operator in the interaction picture can be written as

$$V^\dagger(t, t_0) = V_I^\dagger(t, t_0) V_0^\dagger(t, t_0) = \sum_{n=0}^{\infty} V_n^\dagger(t, t_0) \tag{2.81}$$

where

$$V_n^\dagger(t, t_0) \equiv \left(\frac{i}{\hbar}\right)^n \int_{t_0}^t d\tau_n \int_{t_0}^{\tau_n} d\tau_{n-1} \cdots \int_{t_0}^{\tau_2} d\tau_1 V_0^\dagger(\tau_1, t_0) L'(\tau_1) V_0^\dagger(\tau_2, \tau_1) \times \cdots \\ \times V_0^\dagger(\tau_n, \tau_{n-1}) L'(\tau_n) V_0^\dagger(t, \tau_n). \tag{2.82}$$

The time evolution operators in the Liouville space are directly analogous to those in the Hilbert space, except that the vector in the Liouville space is the density operator instead of wavefunction. Since the time evolution operator, which is a commutator instead of a normal linear operator, describes propagation of both ket and bra vectors in time, the corresponding diagrams in the Liouville space should be different from those in the Hilbert space. The first few terms in the perturbation expansion of $V(t, t_0)$ in Equation 2.79 are now graphically represented as

$$\leftarrow = \leftarrow + \leftarrow \begin{array}{c} \text{wavy} \\ \text{line} \end{array} + \leftarrow \begin{array}{c} \text{wavy} \\ \text{line} \\ \text{wavy} \end{array} + \leftarrow \begin{array}{c} \text{wavy} \\ \text{line} \\ \text{wavy} \\ \text{wavy} \end{array} + \cdots. \tag{2.83}$$

The Hermitian conjugate of $V(t, t_0)$ is then

$$\rightarrow = \rightarrow + \rightarrow \begin{array}{c} \text{wavy} \\ \text{line} \end{array} + \rightarrow \begin{array}{c} \text{wavy} \\ \text{line} \\ \text{wavy} \end{array} + \rightarrow \begin{array}{c} \text{wavy} \\ \text{line} \\ \text{wavy} \\ \text{wavy} \end{array} + \cdots. \tag{2.84}$$

Although the corresponding diagram in the Hilbert space (see Equation 2.34) is identical to a single integral expression, that in the Liouville space is given as a sum of 2^n distinctively different terms for the n th-order perturbation expansion term.